Some properties of two-dimensional inverse energy cascade dynamics

Armando Babiano,[1] Bérengère Dubrulle,[2,3] and Peter Frick[4]
[1]*Laboratoire de Meteorologie Dynamique, ENS, 24, rue Lhomond, 75005 Paris, France*
[2]*CNRS, Service d'Astrophysique, CEA Saclay, L'Orme des Merisiers 709, F-91190 Gif sur Yvette Cedex, France*
[3]*Observatoire Midi-Pyrénées, CNRS URA 285, 14 avenue Belin, F-31400 Toulouse, France*
[4]*Institute of Continuous Media Mechanics, Korolyov street 1, 614061 Perm, Russia*
(Received 7 May 1996; revised manuscript received 12 September 1996)

In this work we analyze the degree of homogeneity and stationarity of the transfers in the inverse energy cascade of two-dimensional turbulence. Two extreme cases, namely, a well-developed inverse energy cascade in a robust statistically steady state and the collision of two vortices of the same sign, which is a clear illustration of a nonstationary cascade regime, are studied. We consider the absolute transfer η_l at scale l produced by the nonlinear term of the Navier-Stokes equation. The scaling properties of the transfer hierarchy $\langle \eta_l^{p+1} \rangle / \langle \eta_l^p \rangle \sim l^{-\delta_p}$ are examined. We define $\Delta = (\delta_\infty - \delta_0)/\zeta_3^*$, where ζ_3^* is the scaling of the third-order structure function of absolute velocity increments, δ_0 is a quantity tracing the smallest but most frequent transfers, and δ_∞ characterizes the largest but rarest transfers. We show that Δ plays a fundamental role in the scaling description of the cascade dynamics. In two-dimensional energy cascade, the important property of the relationship between the scaling of the structure functions and the distribution of the heterogeneities in the physical space given by $(\delta_\infty - \delta_0)$ is the invariance of Δ. Finally, we determine the physical meaning of the formally introduced adjustable parameters in She-Leveque [Phys. Rev. Lett. **72**, 336 (1994)] and Dubrulle [Phys Rev. Lett. **73**, 7 (1994); **73**, 959 (1994)] intermittency models. [S1063-651X(97)11902-X]

PACS number(s): 47.27.−i

I. INTRODUCTION

It is well known that in the inviscid limit as well as in a statistically steady state, the two-dimensional (2D) Navier-Stokes equation is characterized by a family of integral constraints very different from the 3D situation. Basic quadratic invariants in 2D are the kinetic energy and the mean vorticity square (enstrophy). They are both transferred via nonlinear terms in the Navier-Stokes equation from one scale to another following Kolmogorov-Kraichnan's cascade scenario: a direct enstrophy cascade from injection scales toward small dissipative scales, and an inverse energy cascade toward large scales. However, many theoretical and numerical studies [1–5] tend to support the idea that the description of two-dimensional turbulence is not achieved according to the phenomenological theory suggested by Kolmogorov [6,7]. Two-dimensional turbulence can be considered as the synoptic result of a complex distortion process of the velocity field, caused and maintained by the carrying power of long-lifetime coherent structures. The dynamical behavior of two-dimensional turbulence strongly depends on the distribution of coherent vortices, their generation processes, and the stability of their interactions. The phenomenological description of such dynamics remains an open question.

In numerical simulations of two-dimensional turbulence, the relatively large fluctuation of the observed spectral behaviors from one numerical experiment to another, depending on the nature and location of the forcing and dissipation, tend to support the existence of nonuniversal distribution of the active structures participating in the transfers. In other words, for insufficient Reynolds numbers, homogeneity and stationarity is not achieved for relative large scales in the inertial range in which the probability distribution for the velocity increment (structure functions) depend on the large-scale motion and the dissipation. In these situations—this is often the case in practice e.g., in geophysics—, the concept of a local ''homogeneous and stationary continuous inertial cascade'' is not straightforwardly established. An interesting issue, therefore, is to investigate the degree of universality of the transfer dynamics in these cases.

In a recent work [8] we partially analyzed this problem through the investigation of the scaling properties of statistically steady incompressible 2D turbulence using the intermittency model proposed by Dubrulle [9]. This model is a modified version of the model of She and Leveque [10] for 3D turbulence. The modification in Dubrulle's approach takes into account the original idea proposed by Benzi *et al.* [11]. This idea, called ''extended self-similarity'' (hereafter ESS) is to consider the scaling of velocity structure functions under the form

$$\langle |\delta v_l|^p \rangle \propto \langle |\delta v_l|^s \rangle^{\zeta_p/\zeta_s} \tag{1}$$

for all p and s. It generalizes the self-similar scaling of the pth-order moment of the velocity increment δv_l at scale l,

$$\langle \delta v_l^p \rangle \propto l^{\zeta_p}. \tag{2}$$

Experimental investigation of relation (1) in 3D turbulence shows that the relative exponent ζ_p/ζ_s tends to be a scale-independent quantity in the inertial range, even if the absolute exponents ζ_p and ζ_s may depend on l, for example, at low Reynolds number [12]. In [11], the authors concluded that ESS may be ''more fundamental than the self-similar scaling with respect to l usually observed at very high Reynolds numbers.'' From a theoretical point of view, ESS therefore opens possibilities regarding the interpretation and the definition of an ''inertial range.'' An inertial range is physically defined as a range of scales where both the forcing

and the dissipation process are irrelevant. In isotropic homogeneous situations, this implies self-similar scaling of the third-order structure function, and by extension, self-similar scaling of all structure functions. Since neither dissipation, nor forcing explicitly appear in ESS relations like Eq. (1), it could be used for definition of a ''generalized inertial range,'' and therefore enable the definition of scaling exponents in turbulent flows when the deviation from the seminal Kolmogorov's 1941 theory is non-negligible, and the fundamental result $\zeta_3=1$ in the inertial range is not observed. It could be used, for example, in situations where the structure function does not display any evidence of self-similarity with l, such as low Reynolds number experiments [12], or even in certain nonhomogeneous or nonstationary situations. The coincidence of relative scaling exponents computed at low Reynolds number using ESS with relative scaling exponents computed in the usual inertial range at large Reynolds number tends to support this picture. This therefore suggests that ESS could be a natural analyzing tool when investigating certain nonstationary or nonhomogeneous situations. One goal of the present contribution is to explore this issue partially in inverse 2D energy cascade.

Some limitations of ESS have, however, already been detected. Stolovitzky and Sreenivasan pointed out that the ESS property could be limited to low-order moments [13]. Also, recent experimental and numerical investigations have shown that ESS holds in 3D homogeneous and isotropic turbulence both at low and high Reynolds numbers, and for a wide range of scales. However, ESS is not observed in situations when a strong mean shear is present [14], such as in boundary layer turbulence and in the shear behind a cylinder [15]. Our investigation of numerical 2D turbulence showed that ESS is also present there. In Fig. 1 we reproduce the comparison between the absolute exponent ζ_p and the relative exponent ζ_p/ζ_3 in a well-developed inverse energy cascade computed in [8] (the corresponding experiment is called R1024F256 in the present paper). In this experiment, the energy flux defined in Fourier space is constant in the range $0.2\leqslant k/k_I\leqslant 1$, where k_I is the wave number at which forcing occurs; see [8]. This corresponds to a scale interval $1\leqslant l/l_I\leqslant 5$, where $l_I=\pi/k_I$. It is clear that, for low value of p ($p\leqslant 6$), the relative scaling exponents in this interval tends to be scale independent. By contrast, the absolute exponent depends on l. In the light of the previous discussion, this could be seen as a little bit surprising, since large scales are dominated by large vortices generating strong local shear and nonhomogeneous or nonstationary regimes. In two-dimensional turbulence, where vortex interactions are Reynolds number dependent [16], the statistical properties of such regimes are insufficiently known. One goal of the present contribution is to partially explore this issue. We shall show that the ESS property is observed in 2D shear situations.

A goal of the present work is connected with the universality of the scaling exponents. The existence of ESS has led more and more people to focus on ''relative scaling exponents'' such as ζ_p/ζ_3 rather than ''absolute exponents'' such as ζ_p. This interest, first motivated by experimental convenience, was increased when it was discovered that the relative scaling exponents seem to carry a form of universality absent in the absolute scaling exponents: the same set of

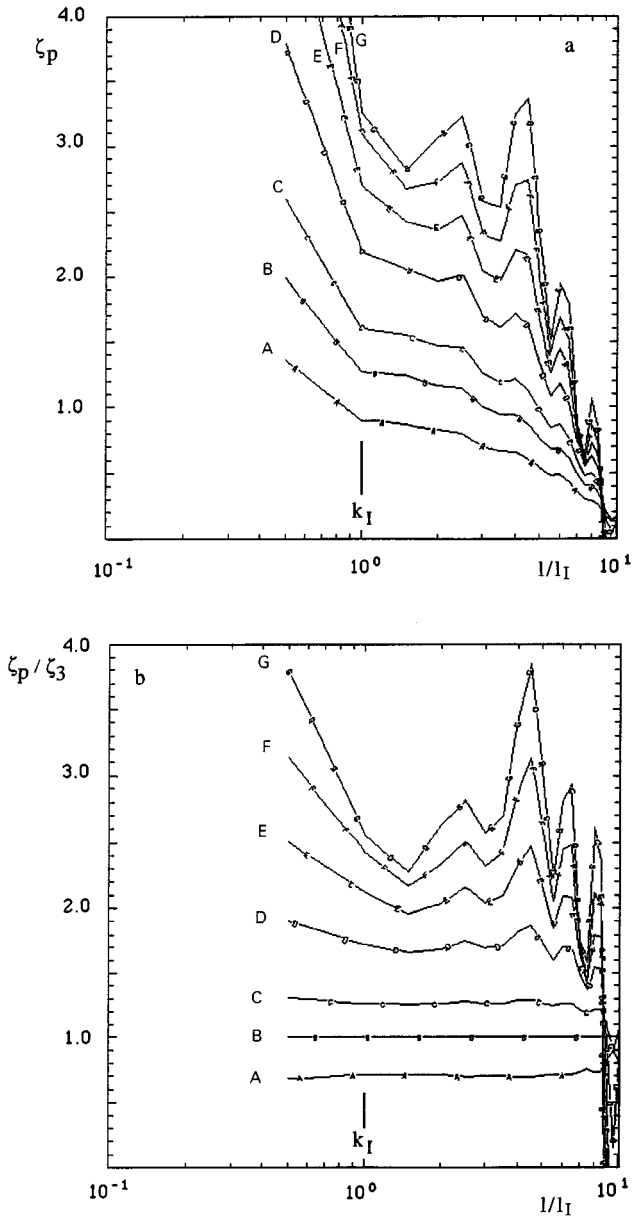

FIG. 1. The absolute exponents (a) and relative exponents (b) as functions of nondimensional scale for increasing values of $p=2(A)$, $3(B)$, $4(C)$, $6(D)$, $8(E)$, $10(F)$, and $12(G)$; l_I is the forcing scale.

relative exponents was observed in 3D turbulence, in Rayleigh-Benard convection in the Bolgiano regime [17], in the solar wind [18], or in Gledzer, Ohkitami, and Yamada (GOY) shell models with different hyperviscosities [19], despite the differences between the absolute scaling exponents. These ''universal values'' are also consistent with the values we measured in the 2D inverse cascade energy range [8]. This could suggest that the relative scaling exponents depends on the conservation laws, but not on the way the turbulence is produced or dissipated.

Motivated by these remarks, we were led to revisit the experimental analysis reported in [8] in order to, on the one hand, unmask the influence of nonhomogeneity, nonstationarity, and shear in the transfers in the inverse energy cascade of two-dimensional turbulence, and, on the other hand, to

investigate the role of the third-order structure function in nonlocal, nonhomogeneous, and nonstationary dynamics. We therefore consider two extreme cases, namely, a well developed inverse energy cascade in a robust statistically steady state and the collision of two signlike vortices, a good illustration of a nonstationary cascade regime. We develop specific tools and a methodology suitable for the analysis of nonlocal, nonstationary, and/or nonhomogeneous situations. These tools are described in Secs. II and III. We shall show that the third-order structure function plays a fundamental role in the scaling description of the 2D energy cascade dynamics. We also determine the physical meaning of the formally introduced adjustable parameters in She-Leveque [10] and Dubrulle [9] intermittency models. Numerical experiments are described in Sec. IV. Our conclusion follows in Sec. V.

II. ANALYZING TOOLS AND METHODOLOGY

The phenomenological theory suggested by Kolmogorov in 1941 [6] to describe the probability distribution for the relative velocities in locally homogeneous and isotropic random velocity fields remains one of most robust approaches in the experimental and theoretical study of developed turbulent flows. The Kolmogorov-Obukhov approach is founded on a relatively simple quantitative description of cascade phenomenon in the inertial range in which the turbulence may be considered locally homogeneous. The basic prediction for the pth-order moment of the velocity increment δv_l at scale l in the energy inertial range is

$$\langle \delta v_l^p \rangle \sim \varepsilon_0^{p/3} l^{p/3}, \tag{3}$$

where ε_0 refers the continuous mean transfer from large scales to small scales. It is constant in this case throughout the cascade, and equal to the mean dissipation rate in the flow domain; $\langle\ \rangle$ refers to averaging over all position vector **x**.

A. Kolmogorov picture and the analysis of turbulence

An important step in the development of relation (3) and of the locally continuous inertial cascade concept is the interpretation and discussion about the Landau critical remark [20] concerning the random nature of the energy dissipation, which is a fluctuating function of the coordinates **x** and time. For insufficient Reynolds number, these fluctuations may depend on the large-scale motion. The refined Kolmogorov similarity hypothesis [7] transforms relation (3) into

$$\langle \delta v_l^p \rangle \sim \langle \varepsilon_l^{p/3} \rangle l^{p/3} \sim l^{\zeta_p}, \tag{4}$$

where now ε_l is the dissipation rate averaged over a spherical volume of radius $l/2$ centered in **x**. Here the scales l are defined in the energy inertial range. A basic ingredient in this phenomenology is the existence of a range of scales (the inertial range) in which the dissipation and the forcing are irrelevant, i.e., the probability distribution of δv_l depends only on the variation of energy per unit time at that scale ε_l and on the scale l:

$$P(\delta v_l) = F(\varepsilon_l, l). \tag{5}$$

Indeed, Eq. (5) could also be recast in different way, namely,

$$\frac{\delta v_l^3}{\langle \delta v_l^3 \rangle} \overset{\text{law}}{=} \frac{\varepsilon_l}{\langle \varepsilon_l \rangle}, \tag{6}$$

where the symbol $\overset{\text{law}}{=}$ here refers to having the same scaling properties,

$$X \overset{\text{law}}{=} Y \Rightarrow \langle X^p \rangle \sim c_p \langle Y^p \rangle, \quad \forall p. \tag{7}$$

Relation (6) is one consequence of Eq. (4). However, Eq. (6) does not necessarily imply relationship (4). Actually, according to Eq. (4) the absolute exponent for structure functions are related by

$$\zeta_p = \frac{p}{3} + \tau_{p/3}, \tag{8}$$

where $\tau_{p/3}$ is the scaling of $\langle \varepsilon_l^{p/3} \rangle$, and characterizes the intermittency correction. Clearly, relation (8) guarantees the basic result $\zeta_3 = 1$ for fully developed, homogeneous, and stationary energy cascade. On the other hand, relation (6) we can deduce that

$$\zeta_p = \frac{p}{3}\ \zeta_3 + \tau_{p/3}^*, \tag{9}$$

where τ_p^* are the scaling exponents of $\langle \varepsilon_l^{p/3} \rangle / \langle \varepsilon_l \rangle^{p/3}$. Relations (8) and (9) only coincide if $\langle \varepsilon_l \rangle$ is constant. In the nonhomogeneous situations studied in the present work, this is not necessarily so, and formulation (9) is better adapted.

One important observation is that the refined similarity hypothesis under form (6) does not predetermine the scaling of third-order structure function. Consequently, relation (6) may be used in situations in which the constraint imposed by homogeneous, infinite Reynolds number and stationary assumptions, i.e.,

$$\lim_{l \to 0} \lim_{\nu \to 0} \lim_{t \to 0} \frac{\langle \delta v_l^3 \rangle}{l} = -\tfrac{4}{5} \langle \varepsilon_l \rangle \tag{10}$$

is violated [see [21] for a detailed discussion of Eq. (10)]. However, we may observe that Eq. (6) is not the only dimensional law compatible with Kolmogorov picture. Relation (6) was first proposed by Dubrulle [9] to account for ESS in some situations. However, it bears a potentially deeper meaning: it guarantees that the partial derivative of the probability distribution with respect to l is zero, and then guarantees the most general requirement for scale symmetry of the probability distribution of δv_l (for more general discussions on the scale symmetry, see, e.g., [22,23]). We may then expect Eq. (6) to hold in a more general context than Eq. (10). Indeed, this form of scaling has been observed in many different flows, from isotropic turbulence to boundary layer, for scales ranging from the integral scales up to the dissipation range [24], i.e., far beyond the range of validity of Eq. (10).

This interesting property makes Eq. (6) the best tool for analyzing flows which are not necessarily homogeneous, isotropic, or stationary, in situations where some form of scale invariance can be expected. To do that, it will be necessary to define more precisely what is exactly meant by the quantity ε_l in Eq. (6). Before that, let us first examine the implication of both similarity hypotheses (4) and (6) to the scaling ζ_p.

B. Link between transfer and velocity increments

She and Leveque [10] and Dubrulle [9] proposed a simple model to describe the intermittency phenomenon in fully developed 3D turbulence. They predict the scaling ζ_p of p-order moments of the velocity increments, and their deviation from behavior (3). Their approach is based on the following hypotheses:

(i) The moments of the energy transfer satisfy the relation

$$\frac{\langle \varepsilon_l^{\,p+1}\rangle}{\varepsilon_l^{\infty}\langle \varepsilon_l^{p}\rangle}\sim\left[\frac{\langle \varepsilon_l^{\,p}\rangle}{\varepsilon_l^{\infty}\langle \varepsilon_l^{\,p-1}\rangle}\right]^{\beta}, \tag{11}$$

where β is a positive constant smaller or equal to 1, and ε_l^{∞} is a normalizing factor which can then be interpreted as the relative contribution to the transfer of the most intermittent structures at scale l. The straightforward development for $p=0,1,2,\ldots,p$ leads to the formula

$$\langle \varepsilon_l^{\,p/3}\rangle\sim\left[\frac{\langle \varepsilon_l\rangle}{\varepsilon_l^{\infty}}\right]^{(1-\beta^{p/3})/(1-\beta)}\varepsilon_l^{\infty p/3}. \tag{12}$$

(ii) In the She-Leveque model, the quantity $\langle \varepsilon_l\rangle/\varepsilon_l^{\infty}$ is given by

$$\frac{\langle \varepsilon_l\rangle}{\varepsilon_l^{\infty}}\overset{\text{law}}{=}\frac{\varepsilon_0}{\varepsilon_l^{\infty}}\sim l^{\alpha}, \tag{13}$$

where ε_0 refers the continuous mean transfer kept constant by the mean dissipation rate at $l\to 0$ in the flow domain. This corresponds to a case where $\langle \varepsilon_l\rangle$ is a scale independent quantity and ε_l^{∞} shows a scale-divergent behavior.

(iii) In Dubrulle's model, the quantity $\langle \varepsilon_l\rangle/\varepsilon_l^{\infty}$ satisfies the relationship

$$\frac{\langle \varepsilon_l\rangle}{\varepsilon_l^{\infty}}\sim\langle \delta v_l^3\rangle^{\gamma}, \tag{14}$$

where γ is an adjustable parameter characterizing the degree of heterogeneity of the transfer field and of the most intermittent structures participating in the transfers.

The combination of Eq. (12) with Eqs. (4) and (13) or (6) and (14) implies that the scaling exponents of the pth-order moment of the velocity increment are given by

$$\zeta_p=\frac{p}{3}[1-\alpha]+\alpha\,\frac{1-\beta^{p/3}}{1-\beta} \tag{15}$$

in the She-Leveque model (in this case $\zeta_3=1$ is imposed), and by

$$\frac{\zeta_p}{\zeta_3}=\frac{p}{3}[1-\gamma]+\gamma\,\frac{1-\beta^{p/3}}{1-\beta} \tag{16}$$

in the Dubrulle model. The identity $\alpha=\gamma$ is of course guaranteed only if $\zeta_3=1$.

Here β and γ are adjustable parameters characterizing the specificity of each flow (conservation laws, forcing, degree of homogeneity). She and Leveque showed that correction (15) is in good agreement with 3D experimental results reported by Benzi *et al.* [11] for $\alpha=\beta=\frac{2}{3}$.

Note that, according to Eq. (12), the deviation from the linear $p/3$ behavior in relation (4) is determined for all p by the value of the adjustable parameter β and the scaling properties of $\langle \varepsilon_l\rangle$ and ε_l^{∞}. If it can be reasonably assumed (as in fully developed turbulence and in continuous cascade scenario) that the lower structure $\langle \varepsilon_l\rangle$ is a scale-independent quantity kept constant by the mean dissipation at $l\to 0$, then correction (12) is determined by β and ε_l^{∞} only. This is the essence of the She and Leveque model. In a more general case, Eq. (12) also depends on the degree of homogeneity of the first moment of the transfer rate $\langle \varepsilon_l\rangle$ and, consequently, on the nonpredetermined scaling properties of $\langle \delta v_l^{\,3}\rangle$. This was implicitly considered in an experimental study [8] in which the ESS property was used in order to obtain a significant improvement in experimental measurements of ζ_p/ζ_3.

As stated in introduction, the existence of ESS may represent more than an experimental tool to compute more precise scaling exponents. In our opinion, it could be viewed as a way to define an ''inertial'' range, even in situations where the exact relation (10) does not necessarily hold. The main goal of the present work is to clarify this problem within formulation (6) and the investigation of the physical meaning of different parameters as γ, β, and ζ_3 in the particular case of nonlocal 2D inverse cascade process.

C. Transfers in 2D inverse cascade

The discussion about the validity of hypotheses (4) or (6) was made in the context of three-dimensional turbulence. In two-dimensional turbulence the situation is more complicated. The condensation of vorticity and energy into coherent vortices depends both on the existence of the energy invariant and on the localness of flow dynamics in physical space [3]. These two fundamental properties of two-dimensional turbulent dynamics are the two most notable ingredients absent in the seminal Kolmogorov's theory. They sustain the concept of the nonuniversality of power laws in the enstrophy and energy inertial ranges. This conclusion is confirmed by results for numerical simulations concerning the enstrophy inertial range reporting nonuniversal energy spectra steeper than the k^{-3} spectrum expected in phenomenological theory. The problem, however, is less prominent in the energy inertial range in which the fate of coherent structures and their contribution to the energy cascade has not yet been adequately studied in numerical simulations. In this case, the viscous dissipation at large scales is negligible in the limit $l\to\infty$, and the statistically steady state is only achieved by the introduction of external friction in the Navier-Stokes equation. The consequence of external artificial large-scale dissipation to the transfer dynamics in the inverse cascade was analysed by Smith and Yakhot [25]. There are situations where both the energy and the enstrophy are transferred toward large scales. The $k^{-5/3}$ spectrum [which is consistent with Eq. (4)] predicted by Kraichnan [26] is observed only in

well-developed forced and dissipated simulations, where the statistically steady state is sufficiently robust [27,28,8]. Recent numerical experiments performed by Borue [29] show, however, an unexpected behavior of the inverse cascade dynamics. These results suggest that there is not much possibility of reaching any robust steady state, and show an anomalous scaling in k^{-3} for the energy spectrum at large scales.

We now return to the interpretation of relation (6), and its adaptation to the 2D inverse cascade problem. Relation (6) means that the third-order velocity structure function and the first moment of the energy dissipation rate have the same statistical properties. This statement contains some contradictions (see, e.g., [21]): first, the right hand side of Eq. (6) refers to a positive value, while the left hand side can have any sign; also, the left hand side concerns the pulsations of velocity—a characteristic of the inertial range—and the right one deals with the dissipation, which, following the definition of the inertial range, is not important at these scales, and become non-negligible only at dissipative scales.

This problem deserves special consideration. Let V_l be a volume (or a surface, in the 2D case) of scale l, laying in the inertial range. The variation of kinetic energy per unit mass in this volume is given by

$$\partial_t E_l = -\frac{1}{V_l}\int_{S_l}(v^2+P)v_n dS - \frac{1}{V_l}\int_{V_l}\varepsilon(x)dV + \frac{1}{V_l}\int_{V_l}q(x)dV. \tag{17}$$

Here S_l is the surface (or contour) of V_l, $\varepsilon(\mathbf{x})$ is the rate of energy dissipation, and $q(\mathbf{x})$ is the rate of energy input by forcing; v_n is the normal component of $\mathbf{v}$ to the surface element (or contour element) dS. Thus

$$\partial_t E_l = -\sigma_l - \varepsilon_l + q_l, \tag{18}$$

where ε_l and q_l are positive, and σ_l can be positive or negative.

Let ε_l be a fluctuating function of the coordinates $\mathbf{x}$ and time,

$$\varepsilon_l = \varepsilon_0 + \varepsilon_l', \tag{19}$$

and $q_l = q_0$ a homogeneous and stationary forcing; ε_0 is the mean dissipation rate, and in any stationary case must be equal to q_0. Thus

$$\partial_t E_l = -\sigma_l + (q_0 - \varepsilon_0) - \varepsilon_l', \tag{20}$$

where both σ_l and ε_l' are sign-changing, scale-dependent values. Note that σ_l is a true inertial range quantity and, in a local dynamics, the latter term concerns the processes operating out of inertial range scales. This description remains true in a 2D inverse cascade process. In this case, the dynamics is nonlocal, and ε_l may be negligible. $\sigma_l = (1/V_l)\int_{S_l}(v^2 + P)v_n dS$, the physical-space energy flux through the surface S_l, is the most important characteristic of the cascade process, especially when the large-scale friction is negligible.

The previous discussion therefore suggests interpreting the quantity ε_l appearing in Eq. (6) as σ_l, which is a true inertial range quantity in local or nonlocal dynamics. Note that this quantity is defined in physical space, and is therefore better suited for investigations in nonhomogeneous situations than the energy flux defined, e.g., in Fourier space.

In our analysis we shall therefore consider that the probability distribution in physical space for the relative velocities in 2D cascade dynamics is basically determined by the absolute contribution to the transfer of the nonlinear term in the Navier-Stokes equation. That is,

$$\eta_l = |\sigma_l|. \tag{21}$$

With this choice, relations (5) and (6) may be rewritten as

$$P(|\delta v_l|) = F(\eta_l, l) \tag{22}$$

and

$$\frac{|\delta v_l|^3}{\langle |\delta v_l|^3 \rangle} \overset{\text{law}}{=} \frac{\eta_l}{\langle \eta_l \rangle}. \tag{23}$$

Note that absolute values of the velocities increments must be chosen to guarantee the consistency of Eqs. (22) and (23), because η_l is the absolute value of energy (or enstrophy) flux through the control surface at scale l. Our choice of the absolute value is essential. Indeed, we assume that $\langle \eta_l \rangle$ contains both the stationary continuous part of the transfer from one scale to another (which will then be the same throughout in the inertial range, and equal to the dissipation rate or forcing rate) and a secondary ''parasite'' scale-dependent localized conservative flux related to the internal shape and the distribution of the structures participating to the transfers. We interpret the ''continuous'' part of the inverse energy transfer as a formation of stable large-scale structures, while the ''parasite'' loops correspond to unstable large-scale structures which decay back. We can assume that the relative number of unstable structures increases with the Reynolds number. This means that the dynamics of the cascade process becomes nonlocal, and depends on larger scales. Taking the absolute value enables us to take into account both above-mentioned contributions, which we believe are both important in determining the shape of the structure functions, i.e., of the probability distribution function $P(|\delta v_l|)$.

Of course, the scaling properties of relations (6) and (23) are equivalent only in the case where:

$$\langle \delta v_l^p \rangle \overset{\text{law}}{=} \langle |\delta v_l|^p \rangle. \tag{24}$$

This is not true in general [30,31]. We show in Sec. IV A that Eq. (24) is well satisfied for $p=3$, but becomes increasingly erronate for larger odd values of p. This shows that our methodology is not strictly equivalent to the model developed by Dubrulle [9], and might be considered a new phenomenology. Note that the good agreement between the model of She and Léveque and experimental results was obtained using the absolute value of velocity increments, which justifies our phenomenology from another point of view.

We may also observe that, in the 2D incompressible case, a similar argumentation could be developed for the variation of the enstrophy per unit mass, in which case η_l would be defined in term of the flux of the square vorticity ω^2 rather

than in term of v^2+P. Dimensionally, relation (6) is unchanged whether one considers ε_l as η_l defined in term of velocity or vorticity. The adoption of one or the other prescriptions depends whether one considers that energy or enstrophy transfers determine the dynamics. In 2D, there could be some ambiguity. We have, therefore, tried both prescriptions. They both appeared to give similar results, but results obtained with the vorticity were slightly less noisy, so we adopted the vorticity prescription. The difference could be induced by the numerical procedure computing $\mathbf{v}$ from ω, since we only solved the barotropic vorticity equation. Therefore, in our experimental investigation, we will define η_l as

$$\eta_l=\frac{1}{l^2}\left|\int_{S_l}\omega^2 v_n dl\right|, \tag{25}$$

where v_n is the normal component of $\mathbf{v}$ to the element dl of the contour S_l containing the control surface at scale l centered on $\mathbf{x}$. For fixed t, we obtained a distribution of values for η_l depending on the position where it is taken. Average values can then be obtained by averaging over all position vectors $\mathbf{x}$.

III. TRANSFER HIERARCHY IN 2D TURBULENCE

We investigate the properties of the transfers by considering the ''absolute transfer'' hierarchy $\langle \eta_l^{p+1}\rangle/\langle \eta_l^p\rangle$. It is bounded by two limits η_l^0 and η_l^∞ defined as

$$\eta_l^0=\lim_{p\to 0}\frac{\langle \eta_l^{p+1}\rangle}{\langle \eta_l^p\rangle}=\langle \eta_l\rangle, \tag{26}$$

$$\eta_l^\infty=\lim_{p\to \infty}\frac{\langle \eta_l^{p+1}\rangle}{\langle \eta_l^p\rangle}. \tag{27}$$

The quantity η_l^0 is equivalent to the mean absolute energy flux, while η_l^∞ characterizes the relative contribution of the most intermittent structures at scale l. Let us now define the following local scaling exponents:

$$\delta_0=-\frac{d\ \ln\eta_l^0}{d\ \ln l}, \tag{28}$$

$$\delta_\infty=-\frac{d\ \ln\eta_l^\infty}{d\ \ln l}. \tag{29}$$

In the inertial range (if any), these two exponents are constant. In the following discussion, it is not necessarily so.

For any values of p, we can parametrize the evolution of the hierarchy as function of p and l as

$$\delta_p=-\frac{d\ \ln\langle \eta_l^{p+1}\rangle-d\ \ln\langle \eta_l^p\rangle}{d\ \ln l}, \tag{30}$$

where δ_p is again a local exponent obeying

$$\delta_p=\delta_\infty+(\delta_0-\delta_\infty)h(p), \tag{31}$$

and $h(p)$ is a monotonous decreasing positive function of p smaller or equal to 1, which, in general, may depend just as well on $(\delta_0-\delta_\infty)$. The parametrization (31) requires that $h(p)$ goes to 1 when p goes to 0, and $h(p)$ goes to 0 when p goes to ∞.

A. Interpretation of δ_0 and δ_∞

The measurement of δ_0 and δ_∞ provides interesting information about the internal shape and spatial repartition of the structures responsible for the transfer. By definition, η_l^∞ characterizes the scaling properties of the structures responsible for the largest, but rarest, transfer. For example, if these structures have a scale-independent shape, $\delta_\infty=0$; if they are very localized structures of characteristic size much smaller than any inertial range scale (e.g., very thin lines extending on scales smaller than the inertial scale), they can be approximated by Dirac functions, and $\delta_\infty=D$, where D is the space dimension (here $D=2$); if they behave like a self-similar singularity with exponent α, then $\delta_\infty=\alpha$; if they are ''regular'' structures (not scale divergent), then $\delta_\infty\leqslant 0$.

By contrast, δ_0 characterizes the structure responsible for the smallest (close to zero) but most frequent transfer. It depends both on the shape and the spatial repartition of these structures. For example, if they are small isolated Dirac peaks, $\delta_0=D$. This is a very inhomogeneous situation. A more homogeneous situation can be obtained with space-filling scale-independent structures. In this case, $\delta_0=0$.

Note that when the transfer is due to only one type of isolated structures, $\delta_0=\delta_\infty$. This is also a nonhomogeneous situation, but it leads to a nonintermittent situation for the velocity structure functions.

We may then single out four special cases: (i) Case A: $\delta_0=\delta_\infty=0$; the transfers are constant and nonintermittent. This situation is the ideal situation considered by $K41$. (ii) Case B: $\delta_0\neq 0$ and $\delta_\infty=\delta_0$; the base of the hierarchy is statistically nonhomogeneous, but the degree of nonhomogeneity does not increase with p. This is a nonhomogeneous and nonintermittent case. (iii) Case C: $\delta_0=0$ and $\delta_\infty\neq\delta_0$; the base of the hierarchy is statistically homogeneous, but there is intermittency. This situation corresponds to the $K62$ situation. (iv) Case D: $\delta_0\neq 0$ and $\delta_\infty\neq\delta_0$; both nonhomogeneity and intermittency prevail. This represents a maximal deviation from the $K41$ hypothesis.

B. Interpretation of $h(p)$

Relations (30) and (31) involve the hierarchy $\langle \eta_l^{p+1}\rangle/\langle \eta_l^p\rangle$ and the scaling limits δ_0 and δ_∞ for all p. The factor $(\delta_0-\delta_\infty)$ is linked to the maximum of amplitude of the intermittency phenomenon in each turbulent flow, whereas $h(p)$ refers to the corresponding correction as function of p. Clearly, if $h(p)=1$ for all p, the correction introduced by Eq. (31) comes only from the basic properties of $\langle \eta_l\rangle$.

The simplest function which satisfies the constraints on $h(p)$ is

$$h(p)=e^{-ap}, \tag{32}$$

where $a=h'(0)$ characterizes the steepness of $h(p)$ at $p=0$, i.e., the properties of the transfer hierarchy at moderate values of p. Using Eq. (31), the first derivative $h'(0)$ is defined by $\delta_p'(0)$. We obtain

$$a=\frac{\delta_p'(0)}{\delta_\infty-\delta_0}. \tag{33}$$

Clearly, since $\delta_p'(0)\geqslant 0$, we have $a\geqslant 0$.

On the other hand, simple manipulation shows that, for every values $\delta_\infty\neq\delta_0$, hierarchies (30) and (31) verifies the relation

$$\frac{\langle \eta_l^{p+1}\rangle}{\eta_l^\infty\langle \eta_l^{p}\rangle}\sim\left[\frac{\langle \eta_l^{p}\rangle}{\eta_l^\infty\langle \eta_l^{p-1}\rangle}\right]^{h(p)/[(p-1)]} \tag{34}$$

Note that, if $\delta_\infty=\delta_0$ (or $\delta_\infty\to\delta_0$), then $h(p)/h(p-1)=1$ [or $h(p)/h(p-1)\to 1$]. We see that Eq. (34) is consistent with the hierarchy (11) postulated by She and Leveque [10], provided that $h(p)$ have been defined in the frame of the approximation (32). That is,

$$\frac{h(p)}{h(p-1)}=\beta=e^{-a}, \tag{35}$$

both scale and p independent. Here the physical meaning of the adjustable parameter in intermittency models [10] and [9] β is established: under assumption (32), β is determined by Eqs. (33) and (35).

Dubrulle [9] and She and Waymire [32] showed that relation (11) with constant β holds when the probability density function for ε_l is a log-Poisson distribution (see, for example, [33] for experimental discussion in the shell models). We see that this is, strictly speaking, a simplifying assumption which results only from the approximations (32) and (35). In this sense, the log-Poisson model is only the simplest modelization of the hierarchy. More complex hierarchies result in nonconstant $h(p)/h(p-1)$ (see examples in [32,22] or in Sec. IV). Note, however, that for large enough, the hierarchy $\langle \eta_l^{p+1}\rangle/\langle \eta_l^{p}\rangle$ saturates toward the limit η_l^∞. According to Eqs. (32) and (33), finally, we see that the adjustable parameter β in the simplest approximation (log-Poisson distribution) is defined by $h'(0)$, δ_0, and δ_∞. The property that β may be universal in the frame of given conservation laws in nonhomogeneous and/or nonstationary situations is therefore not guaranteed.

C. Achievement of ESS

We can now establish the link between absolute transfer and velocity increments. From hierarchies (30) and (31), the straightforward development for $p=0,1,2,\ldots,p$ leads to the formula

$$\frac{\langle \eta_l^{p}\rangle}{\langle \eta_l\rangle^p}\sim l^{(\delta_\infty-\delta_0)[I(p)-p]}, \tag{36}$$

where $I(p)$ is the function

$$I(p)=\sum_{q=0}^{p-1}h(q). \tag{37}$$

If Eq. (23) holds, the exponents of the absolute velocity structure functions

$$\langle|\delta v_l|^p\rangle\sim l^{\zeta_p^*} \tag{38}$$

can be expressed using the functions $I(p)$, δ_0, and δ_∞ introduced above. They are

$$\frac{\zeta_p^*}{\zeta_3^*}=\frac{p}{3}\left[1-\frac{(\delta_\infty-\delta_0)}{\zeta_3^*}\right]+\frac{(\delta_\infty-\delta_0)}{\zeta_3^*}I(p/3), \tag{39}$$

For example, assuming the simplest approximation $h(p)=\beta^p$ and $I(p)=(1-\beta^p)/(1-\beta)$, one recovers formula (16) applied to exponents of the absolute velocity increments. The important observation is that formula (39) for the relative scaling exponents ζ_p^*/ζ_3^* is obtained without the ESS assumption (1). We see that the relative exponents only depends on $I(p)$ and on the statistical properties of the quantity

$$\Delta\equiv\frac{(\delta_\infty-\delta_0)}{\zeta_3^*}. \tag{40}$$

The scale independence of the relative exponents, i.e., ESS, is guaranteed, provided only both $I(p)$ and Δ are scale independent. The first property is linked with the existence of a well-defined ''hierarchy.'' The second property has been observed, for example, in well developed 3D isotropic turbulence, Rayleigh-Benard convection [24], or in shell models with hyperviscosities [19]. In all these cases, Δ appears to be about two-thirds, predicted by She and Leveque [10]. A fit with experimental measurements of Benzi *et al.* [11] gives $\Delta=0.82$ [36]. In systems with different conservation laws, such as shell models [33] or in the 2D enstrophy cascade [8], Δ is different from this value. In the enstrophy cascade $\Delta\approx 0$ (no intermittency), but in the inverse energy cascade, we found $\Delta\approx 0.47$ [8]. From all these experimental results one may speculate that Δ appears as a universal quantity (i.e., independent of the mean dissipation, flow geometry, stationarity, or homogeneity) in the energy cascade range. If Δ is a universal scale-independent quantity in the energy range, identity (40) justifies the universality of the relationship

$$\langle|\delta v_l|^3\rangle\sim\left(\frac{\eta_l^0}{\eta_l^\infty}\right)^{1/\Delta}, \tag{41}$$

which is consistent with the Dubrulle's assumption (14) if $\langle \delta v_l^3\rangle$ and $\langle|\delta v_l|^3\rangle$ have same scaling properties. The interesting conclusion is that the ESS property is generically linked with the validity of relationship (41) in the inertial range. Note that the universality of Δ does not implie in precise way the universality of the relative scaling exponents. They also depend on the complexity of $I(p)$.

Relation (41) may be rewritten as

$$\frac{\langle|\delta v_l|^3\rangle}{l}\sim\varepsilon_0\left(\frac{l}{l_I}\right)^{(\delta_\infty-\delta_0-\Delta)/\Delta}, \tag{42}$$

where ε_0 is the input rate at scale l_I. If $\langle \delta v_l^3\rangle\overset{\text{law}}{=}\langle|\delta v_l|^3\rangle$, this relation appears as a generalization (to nonhomogeneous situations) of both K41 and K62 phenomenology based on the exact result (10) valid for locally homogeneous and stationary turbulence. In the first case, $\delta_\infty=\delta_0=0$ and $\Delta=0$; in the second case, $\delta_0=0$ and $\delta_\infty=\Delta$, so that both formulas lead to $\zeta_3^*=1$. Otherwise, $\delta_0\neq\delta_\infty\neq 0$, and we observe that Eq. (42) tends to exact result (10) only if $(\delta_\infty-\delta_0)$ tends to Δ.

It is therefore interesting to evaluate the behaviors of Δ, $I(p)$, and $(\delta_\infty - \delta_0)$ in various nonhomogeneous or nonstationary situations, with given conservation laws. In Sec. IV we present an experimental study of Δ, $I(p)$, and $(\delta_\infty - \delta_0)$ in different 2D energy cascade situations, namely, a statistically steady well-developed energy cascade and a nonstationary vortex interaction.

IV. EXPERIMENTAL RESULTS

We use the classical simulation of stationary incompressible two-dimensional turbulence solving the barotropic vorticity equation on a periodic square domain $(2\pi,2\pi)$, using a pseudospectral scheme. We consider some experiments which were already analyzed in [8]:

(i) An experiment at a resolution of 1728×1728 with a forcing at wave number $k_I=40$. In this simulation, both the inverse cascade of energy and direct cascade of enstrophy can be studied (experiment R1728F40).

(ii) An experiment at a resolution 1024×1024 with a forcing at a large wave number $k_I=256$. This simulation presents a well-developed inverse cascade of energy (experiment R1024F256).

(iii) An experiment at a resolution 128×128 unreported in [8], with a forcing at wave number $k_I=10$. This simulation does not present any signature of a developed inverse energy cascade, and will be used to analyze the interaction of the same sign vortices (experiment R128F10).

Here we consider a situation in which the two-dimensional incompressible turbulence is forced by a stationary force whose spectrum is concentrated in a neighborhood of the wave number k_I, and in which a robust statistically steady state is reached: the forcing which is defined by keeping the amplitude of the mode k_I constant in time is compensated for by the dissipation at small and large scales. In all our simulations, a linear friction at largest scales was used. In R1728F40 and R128F10 experiments, the dissipation at small scales was parametrized by the hyperviscosity method. In the R1024F256 experiment, where the cutoff scale is of the order of the input scale, the anticipated potential vorticity method was used [34]. The energy spectra are displayed in Fig. 2 (other information concerning these simulations and more extensive analysis of corresponding energy spectra, energy, and enstrophy fluxes in Fourier space, and structure functions characterizing these fields, can be found in our previous studies [8,28,35]). The vortex interaction is analyzed in the R128F10 experiment in a 41×41-grid-interval subdomain (i.e., 2.2 times the most energetic scales) centered on one of the vortices. The motion of the subdomain is experimentally studied with a Lagrangian monitoring of the vortex epicenters. The vortex interaction is a nonstationary turbulent event. The Reynolds numbers in these simulations are close to 800 (R1728F40), 500 (1024F256), and 60 (R128F10). In all three turbulent fields coherent structures are present.

A. Transfer hierarchy: Stationary state

Here we analyze the high-resolution simulations R1728F40 and R1024F256 in the statistically steady state. In the R1728F40 experiment both the energy and enstrophy cascades are resolved. We observe a close to $k^{-5/3}$ and $k^{-3.5}$ spectra in the energy and enstrophy ranges, respectively. In the R1024F256 experiment, a well-developed $k^{-5/3}$ inverse cascade of energy is resolved.

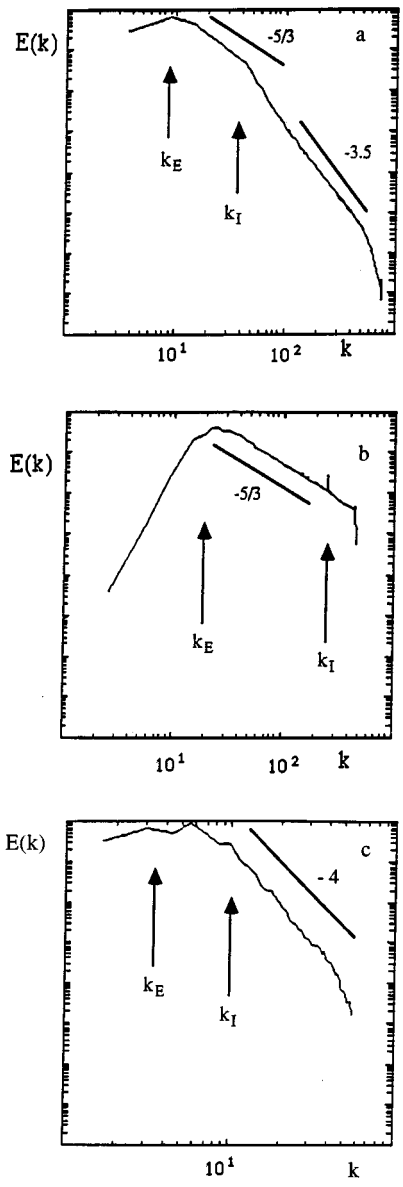

FIG. 2. Energy spectra as function of wave number k. Arrows indicate the injection wave number k_I and the most energetic wave number k_E; experiments R1728F40 (a), R1024F256 (b), and R128F10 (c).

1. Comparison between $\langle \delta v_l^p \rangle$ and $\langle |\delta v_l|^p \rangle$

We have performed a comparison between $\langle \delta v_l^p \rangle$ and $\langle |\delta v_l|^p \rangle$ for odd values $p=1$, 3, 5, and 7. The result is displayed in Fig. 3. It can be seen that the scaling properties of the two quantities nearly coincide for $p=3$ in large interval, but increasingly differ for $p>3$. This shows that $\zeta_3=\zeta_3^*$, but $\zeta_p \neq \zeta_p^*$ for $p>3$.

2. Transfer hierarchy

The experimental illustration of the transfer hierarchy $\langle \eta_l^{p+1} \rangle / \langle \eta_l^p \rangle$ as a function of nondimensional scale

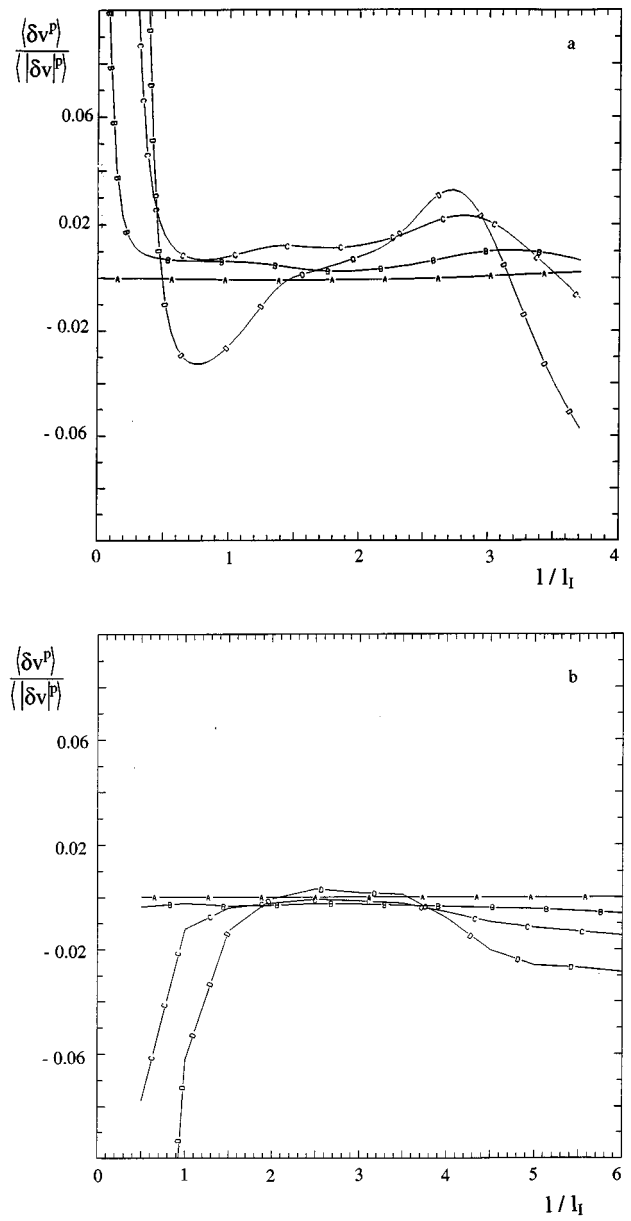

FIG. 3. Comparison between $\langle \delta v_l^p \rangle$ and $\langle |\delta v_l|^p \rangle$ for $p=1(A)$, $3(B)$, $5(C)$, and $7(D)$; experiments R1728F40 (a) and R1024F256 (b).

l/l_I ($l_I=\pi/k_I$) for increasing values of p (up to $p=12$) is reported in Figs. 4(a) (R1728F40) and 4(b) (R1024F256). It is quite clear that formulations (30) and (31) is well supported. From Fig. 4(a) we observe two different scaling properties of the transfer hierarchy as a function of l and p. In the enstrophy range ($l/l_I \leqslant 1$), the hierarchy shows a behavior which is consistent with case B described in Sec. III namely, $\langle \eta_l \rangle$ is statistically nonhomogeneous ($\delta_0 \neq 0$), and the degree of nonhomogeneity does not increase with p ($\delta_\infty \approx \delta_0$). This result confirms the weak degree of intermittency characterizing the direct enstrophy cascade dynamics in the robust stationary situation [8]. Note also that the scaling of the transfer hierarchy is close to l^{-1} ($\delta_0 \approx 1$) and that the case $\delta_\infty = D$ is not reached in this range. It thus seems that the very crude growth of p preserves the repartition of rarest and frequent transfer in the enstrophy cascade.

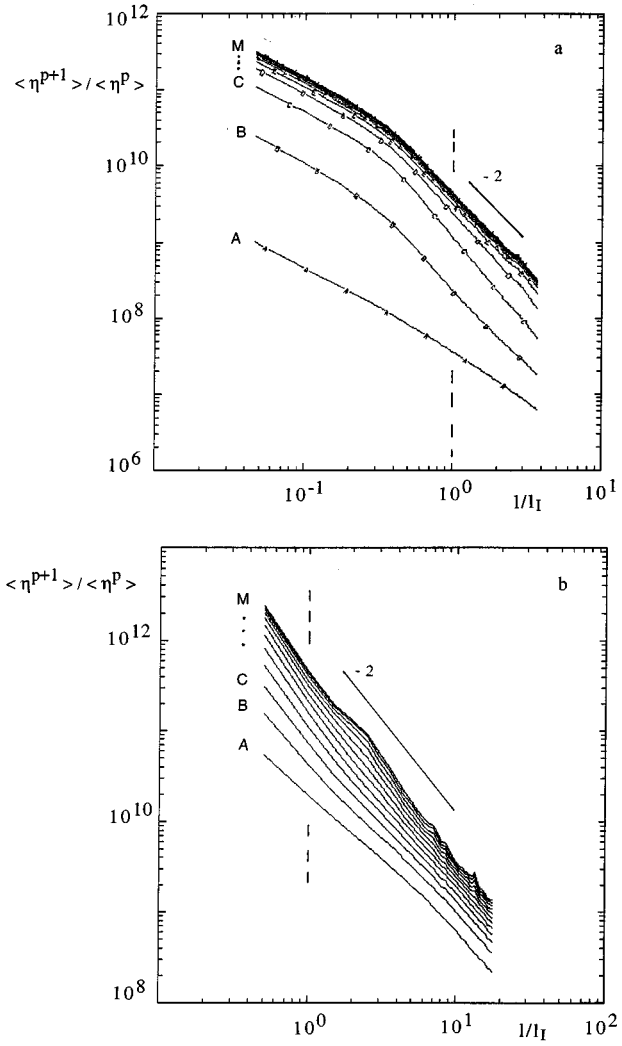

FIG. 4. The transfer hierarchy as function of nondimensional scale for $p=0(A)$, $1(B)$, $2(C),\ldots,12(M)$; experiments R1728F40 (a) and R1024F256 (b).

In the energy interval ($l/l_I \geqslant 1$), we observe a very different behavior with a strong sensitivity of the hierarchy shape for moderate values of p. For $p=0$, the underlying shape is $l^{-4/3}$ ($\delta_0 \approx \frac{4}{3}$). As p increases, the slope rapidly converges to a strongly nonhomogeneous situation characterized by $\delta_\infty = D$ (isolated Dirac peaks). This process in the energy interval corresponds to case D described in Sec. III, and is as well confirmed by the R1024F256 experiment [Fig. 4(b)]. We see that in both simulations the underlying shape is characterized by $\delta_0 \approx \frac{4}{3}$, and the strongly nonhomogeneous threshold by $\delta_\infty = D$.

3. Behaviors of Δ, ($\delta_\infty - \delta_0$), and ζ_3^*

The experimental illustration of the behaviors of Δ, $(\delta_\infty - \delta_0)$, and ζ_3^* as function of nondimensional scale l/l_I in the well-developed inverse energy cascade F1024R256 is reported in Fig. 5. According to the spectrum behavior in $k^{-5/3}$, the exponent ζ_3^* remains close to 1 for $l/l_I \geqslant 1$ (it tends to 3 when $l/l_I \to 0$, see [2]). We observe that the scale dependency of ζ_3^* and $(\delta_\infty - \delta_0)$ remains correlated throughout the whole energy interval $1 \leqslant l/l_I \leqslant 5$ resolved in this experiment. As a

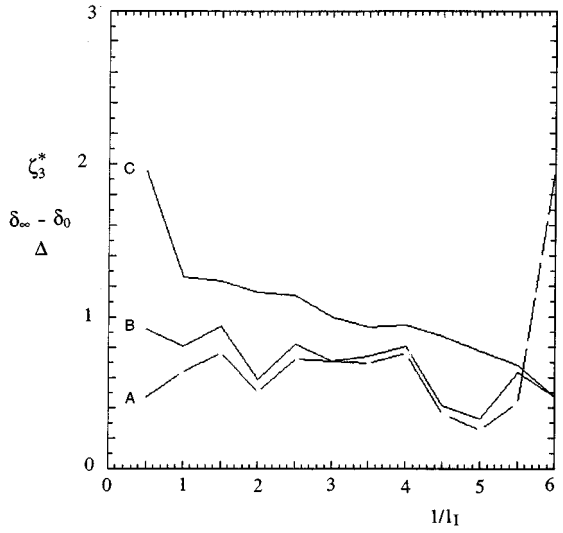

FIG. 5. The behaviors of Δ (A), $(\delta_\infty-\delta_0)$ (B), and ζ_3^* (C) as functions of nondimensional scale; experiment F1024R256.

result, Δ appears as scale-independent quantity in well developed and stationary inverse cascade dynamics. From Fig. 5 we may conclude that the value of Δ is between 0.7 and 0.8, as in the fit performed in [36] for three-dimensional turbulence, but slightly above the value $\frac{2}{3}$ from the model of She and Leveque.

4. Relative exponents

The only difference between the two behaviors for the hierarchy $\langle \eta_l^{p+1}\rangle/\langle \eta_l^p\rangle$ in the energy range (Fig. 4) is that in R1024F256 experiment the value of $\delta'(0)$ is smaller than in R1728F40 experiment, in spite of the fact that in both cases we observe identical underlying shape δ_0 and strongly nonhomogeneous threshold δ_∞. The measured values of δ_p, the parameter a defined by Eq. (33), and the corresponding $\beta=e^{-a}$ in the log-Poisson approximation can be found in Table I. In the R1728F40 experiment, $\delta'(0)=0.93$ ($\beta=0.3$), whereas, in the R1024F256 experiment, $\delta'(0)=0.2$ ($\beta=0.7$).

This experimental observation indicates that $h(p)/h(p-1)=(\delta_p-\delta_\infty)/(\delta_{p-1}-\delta_\infty)$ depends on p, and that functions $h(p)$ and $I(p)$ do not only depend on the conservation laws. In this case, the parameter β in the log-Poisson approximation appears as a nonuniversal quantity. One may then question whether, under such conditions, the log-Poisson approximation indeed has any practical significance.

B. Transfer hierarchy: Nonstationary regime

As pointed out in [1] and [3], the collision of two vortices of the same sign, which produces a coalescence into a single vortex, is a clear illustration of the inverse energy cascade. The two interacting vortices turn around each other, getting closer and closer until they finally aggregate in a vortex. In the nonstationary regime, the resulting vortex has a larger scale than two incident vortices. Conversely, if the external constraints (forcing and dissipation) generate a robust steady state, then after some relaxation time the vortex tends to recover the scale of incident vortices. This process has a nonstationary character. The various panels of Fig. 6 show the vorticity levels in a 41×41 grids interval subdomain during a typical collision of two vortices of the same sign (experiment R128F10). Figure 7 shows the enstrophy (a) (averaged in the 41×41 grid interval subdomain) and the integral $\Pi=\int\langle \eta_l\rangle dl$ defined over energy cascade scales (b) as function of time. During the collision of two vortices ($2.3<t<2.4$) these quantities increase to a maximum value, and after a transient regime they become stabilized around a stationary value. The energy and enstrophy were thus normalized by the stationary values in the steady state, namely, $E=53$ and $Z=2500$, respectively, in the R128F10 experiment. The maximum of the enstrophy in the Fig. 7(a) defines a local eddy-turnover times close to 0.028. From our experimental study we may estimate that the length of the collision of two vortices is close to 11 local eddy-turnover times. Prescribing the forcing scale to be 50 km and the mean kinetic energy to be 12.5 $cm^2\ s^{-2}$ (the ocean dynamics parameters, for example) we obtain the time-scale factor $t^+=330$ days and the space-scale factor $l^+=159$ km. We may estimate that the length of this nonstationary inverse cascade regime linked to the collision of two vortices in the ocean context is close to 100 days.

We shall illustrate our analysis in two different contexts: (i) a time-averaged computation in all stationary interval $2.7<t<3.3$; and (ii) a time-averaged computation around $t=2.4$, which we may consider the most active episode characterizing the collision of two vortices.

1. Transfer hierarchy

Figures 8(a) and 8(b) show the transfer hierarchy as function of nondimensional scale $l/l_I(l_I=\pi/k_I)$ for increasing values of p (up to $p=12$) in the cases defined above. Case (i) is showed in Fig. 8(a). We indeed recover in this elementary event the same basic properties already unmasked in high-resolution simulations and well-developed cascade dynamics, namely, $\delta_0\approx\frac{4}{3}$ and $\delta_\infty=D$. Clearly, in this case, the energy interval is very short.

Case (ii) is shown in Fig. 8(b). We see that the threshold δ_∞ remains unchanged, whereas the underlying shape δ_0 decrease from $\frac{4}{3}$ to a value close to 0.7 during the most active episode characterizing the collision of two vortices. This shows that parameter δ_∞ is a stationary function at times, i.e., during the interaction of two vortices, the repartition of rarest but largest transfer is stationary. In contrast, δ_0 may change in time. It seems that the vortex interaction tends to favor locally the homogeneous repartition of the smallest but most frequent transfers at energy cascade scales ($\delta_0\to0$).

2. Behaviors of Δ, $(\delta_\infty-\delta_0)$, and ζ_3^*

What is the evolution of Δ in this case? Figure 9 shows Δ, $(\delta_\infty-\delta_0)$, and ζ_3^* in computation (ii). The value of ζ_3^* in the

TABLE I. Measured values of δ_p, a, and β.

Experiment	δ_0	δ_1	δ_2	δ_3	δ_4	δ_5	δ_6	a	β
R1728F40	1.3	2.23	2.2	2.1	2	2	2	1.281	0.278
R1024F256	1.4	1.6	1.66	1.7	1.7	1.8	2	0.333	0.716
R128F10(i)	1.25	1.95	2	2	2	2	2	0.933	0.393
R128F10(ii)	0.7	1.95	2	2	2	2	2	0.961	0.382

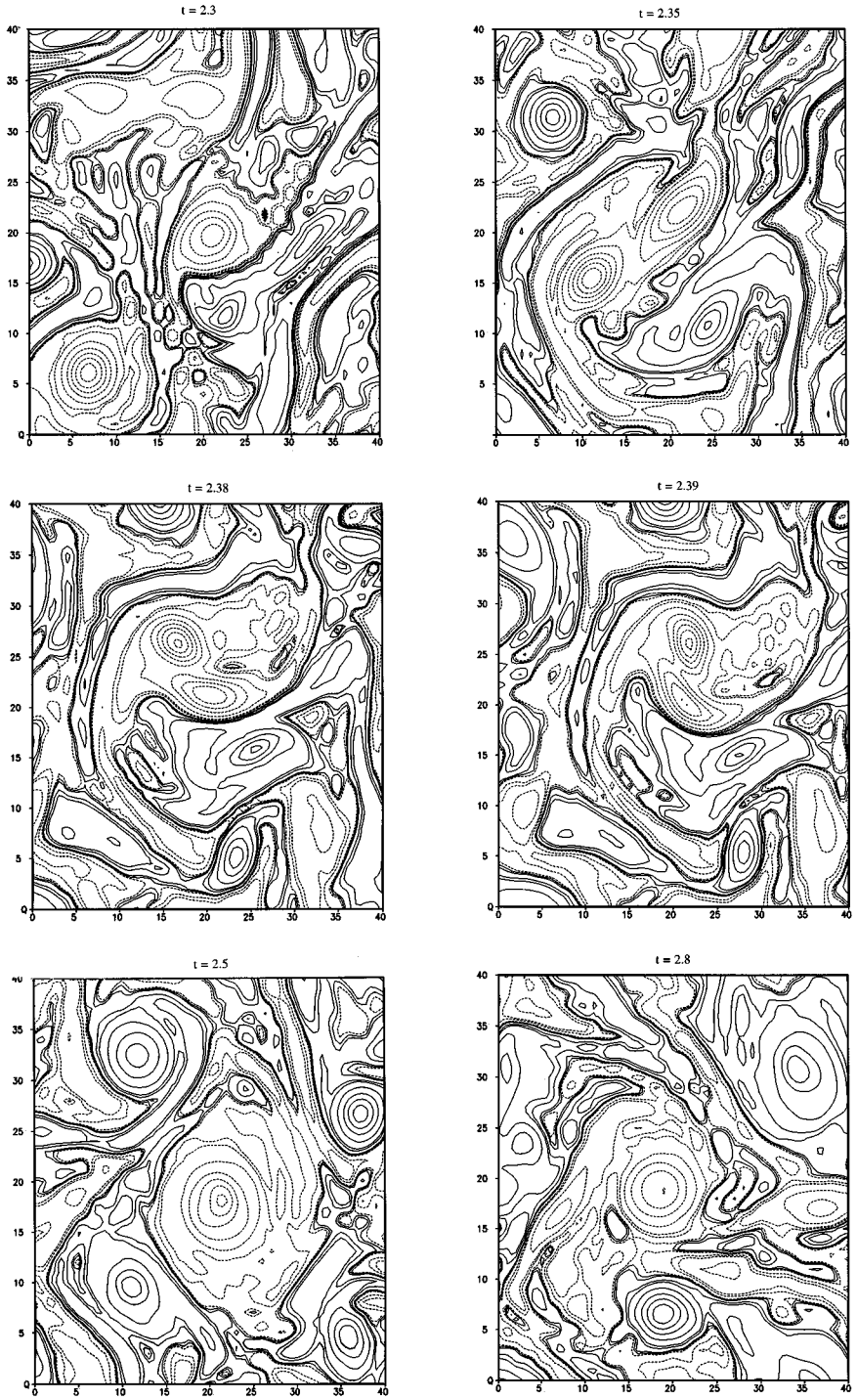

FIG. 6. Time evolution of the vorticity levels during the collision of two vortices of the same sign in a 41×41 grid interval subdomain for the R128F10 experiment. The images correspond to the times $t=2.3$, 2.35, 2.38, 2.39, 2.5, and 2.8.

short developed energy interval $1 \leqslant l/l_I \leqslant 1.3$ is in this case close to 1.6. However, this anomalous large value of ζ_3^* is compensated for by $(\delta_\infty - \delta_0)$, and Δ remains unchanged and close to the value between to 0.7 and 0.8 observed in the stationary situation (see Fig. 5). This result does not implies in general way the universality of Δ. The interesting observation is that Δ appears as a scale-independent stationary function at time in the energy interval as the nonhomogeneous threshold δ_∞. This shows that the scaling properties of $\langle |\delta v_l|^3 \rangle$ and δ_0 remain correlated in time, even if the evolution of the turbulence have a nonhomogeneous and nonstationary character.

3. Relative exponents

Figure 10 shows the comparison between the relative exponents ζ_p^*/ζ_3^* for $p=2$, 4, and 6 as function of nondimensional scale l/l_I in the stationary passive period [case (i)] and in the nonstationary regime during the collision of two vor-

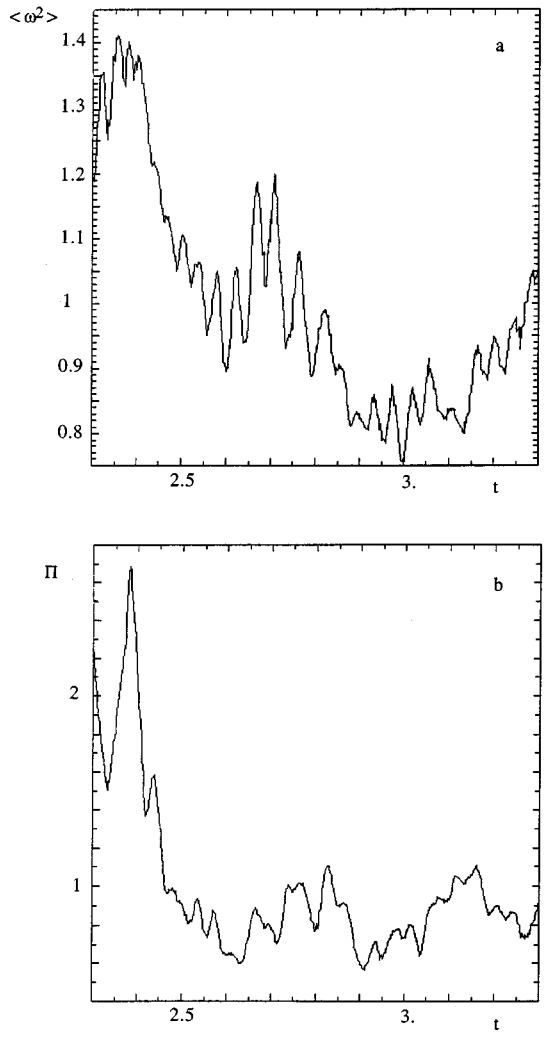

FIG. 7. The enstrophy (a) and the transfer integral $\Pi=\int\langle\eta_l\rangle dl$ (b) during the collision of two vortices; experiment R128F10.

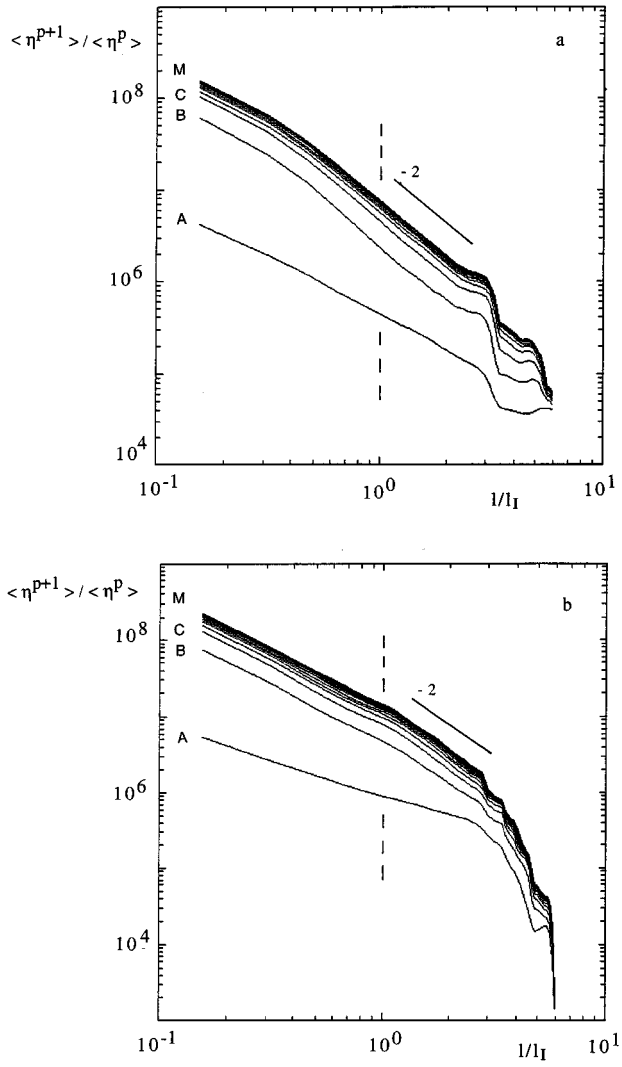

FIG. 8. The transfer hierarchy as function of nondimensional scale for $p=0(A)$, $1(B)$, $2(C),\ldots,12(M)$; (a) stationary interval [case (i)], (b) nonstationary regime [case (ii)]. Experiment R128F10.

tices [case (i)]. We observe in case (ii) that the collision favors the definition of the relative exponents in a largest interval $l/l_I>1$, and ESS is present in the same way for $p=6$. In spite of the low Reynolds number, this is probably consistent with the fact that the vortex interaction tends to make the mean transfer more homogeneous. By contrast, in case (i) ESS is present only for $p=2$. Note that the important result is that the relative exponents in these two different situations are comparable in spite of the fact that $(\delta_\infty-\delta_0)_{(i)} \neq(\delta_\infty-\delta_0)_{(ii)}$. This confirms the low variability of Δ as function of time and of the spatial repartition of the structures responsible for the smallest but most frequent transfers.

Finally, the measured values of δ_p, the parameter a defined by Eq. (33), and the corresponding $\beta=e^{-a}$ can be found in Table I. Note that, in both experiments, $a=0.933$(i) and 0.961(ii), $\beta=0.393$(i) and 0.382(ii), and $h(p)/h(p-1)=(\delta_p-\delta_\infty)/(\delta_{p-1}-\delta_\infty)$ do not depend on p.

V. CONCLUSION

Here we summarize our main results: a self-consistent methodology, generalizing Kolmogorov's approach, has been developed to study nonhomogeneous and/or nonstationary turbulent situations. This methodology also includes the She and Leveque and Dubrulle intermittency models, and provides a physical interpretation of the parameters appearing in these models. It has been applied on two cases drawn from 2D turbulence: in the inverse energy cascade regime, where the presence of strong vortices induces a nonhomogeneous situation, and in the interaction of two vortices, a nonstationary situation.

Our analysis has revealed a number of interesting facts.

(i) The limits of the log-Poisson description; in the present case, it appears unsupported even in the stationary regime. It could therefore be a peculiarity of homogeneous situations.

(ii) The existence of a scale-independent stationary parameter Δ, connected with the existence of ESS. This parameter, including the influence of inhomogeneities and cascade properties, seems to depend mostly on conservation laws, but not on the existence of an inertial range ''a la Kolmogorov'' ($\zeta_3=1$), nor on the presence of inhomogeneities or on nonstationary effects. These properties of Δ open possibilities

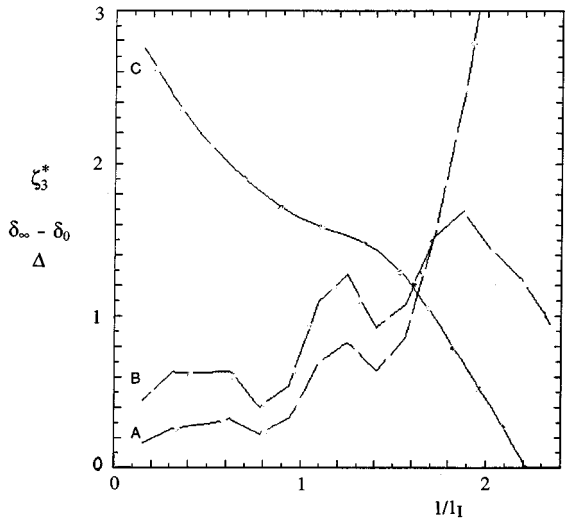

FIG. 9. The behaviors of Δ (A), $(\delta_\infty - \delta_0)$ (B), and ζ_3^* (C) as functions of nondimensional scale during the collision of two vortices; experiment F128R10 [case (ii)].

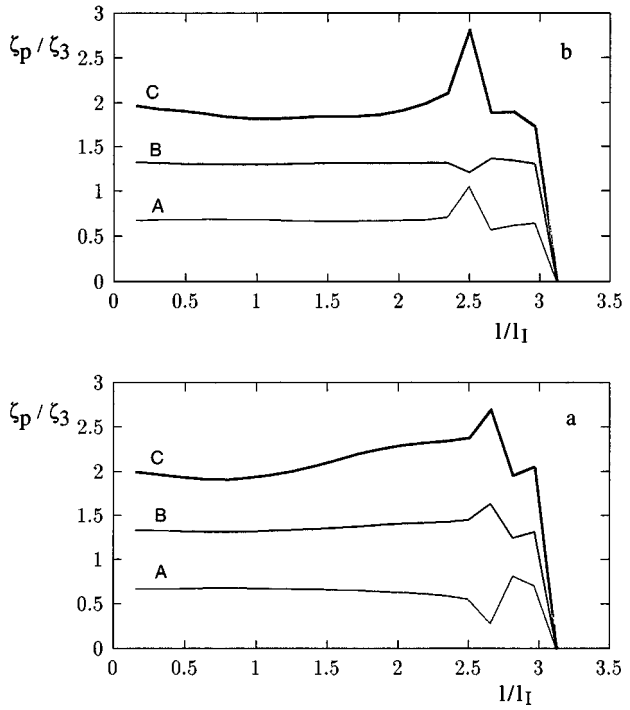

FIG. 10. The relative exponents as function of nondimensional scale for increasing values of $p=2(A)$, $4(B)$, and $6(C)$; (a) case (i), (b) case (ii). Experiment R128F10.

regarding the phenomenological description of the two-dimensional turbulent dynamics, and suggest an interesting interpretation of some unexpected results of the numerical simulations mentioned previously. For example, we have observed that vortex interactions tend to make the mean transfer more homogeneous ($\delta_0 \to 0$), while keeping unchanged the structure of the rarest events ($\delta_\infty = cte = 2$ and $a \to 1$). In the extreme situation of a large-scale structure made only of interacting vortices, one may then expect $\delta_0 \approx 0$, $\delta_\infty = 2$, and $\beta = 0.37$. Since Δ does not depend on nonstationary effects, $\Delta \approx 0.7$. From Eqs. (40) and (39), $\zeta_3 \approx 3$ and $\zeta_2 \approx 2$, i.e., a k^{-3} energy spectra in the inverse cascade as in Borue's numerical experiments [29].

(iii) The nonuniversality of relative scaling exponents, due the nonuniversality of the transition from mean to rarest transfer events.

Finally, the universality of Δ is generically linked with relationship (42), which appears as a generalization to nonhomogeneous and nonstationary turbulence of the classic Kolmogorov's approach. The analysis developed in this work is basically supported by specific properties of numerical experiments. The other problem is the investigation of our methodology in laboratory or *in situ* experiments or in the framework of 3D turbulent dynamics.

[1] J. C. McWilliams, Fluid Mech. **146**, 21 (1984).
[2] A. Babiano, C. Basdevant, and R. Sadourny, J. Atmos. Sci. **42**, 941 (1985).
[3] A. Babiano, C. Basdevant, B. Legras, and R. Sadourny, J. Fluid Mech. **183**, 379 (1987).
[4] P. Santangelo, R. Benzi, and B. Legras, Phys. Fluids A **1**, 1027 (1987).
[5] K. Ohkitani, Phys. Fluids A **3**, 1598 (1991).
[6] A. N. Kolmogorov, C. R. Acad. Sci. USSR **30**, 299 (1941).
[7] A. N. Kolmogorov, J. Fluid Mech. **13**, 82 (1962).
[8] A. Babiano, B. Dubrulle, and P. Frick, Phys. Rev. E **52**, 4 (1995); **52**, 3719 (1995).
[9] B. Dubrulle, Phys. Rev. Lett. **73**, 7 (1994); **73**, 959 (1994).
[10] Z.-S. She and B. Leveque, Phys. Rev. Lett. **72**, 336 (1994).
[11] R. Benzi, S. Ciliberto, R. Tripiccione, C. Baudet, F. Massaioli, and S. Succi, Phys. Rev. E **48**, 1 (1993); **48**, R29 (1993).
[12] M. Briscolini, P. Santangelo, S. Succi, and R. Benzi, Phys. Rev. E **50** 1795 (1994).
[13] G. Stolovitzky and K. R. Sreenivasan, Phys. Rev. E **48**, 1 (1996); **48** R33 (1996).
[14] R. Benzi, M. Struglia, and R. Tripiccione, Phys. Rev. E **53**, R5565 (1996).
[15] R. Benzi, S. Ciliberto, C. Baudet, G. Ruiz, and R. Tripiccione, Europhys. Lett. **24**, 275 (1993).
[16] D. Dritschel and N. Zabusky, Phys. Fluids **8**, 1252 (1996).
[17] R. Benzi, R. Tripiccione, F. Massaioli, S. Succi, and S. Ciliberto, Europhys. Lett. **25**, 331 (1994).
[18] R. Grauer, Phys. Lett. A **195**, 335 (1994).
[19] E. Leveque and Z. S. She, Phys. Rev. Lett. **75**, 2690 (1995).
[20] L. D. Landau and E. M. Lifschitz, *Fluid Mechanics*, 2nd ed. (Pergamon, Oxford, 1987).
[21] U. Frisch, *Turbulence* (Cambridge University Press, Cambridge, 1995).
[22] B. Dubrulle and F. J. Graner, Phys. (France) II (to be published).
[23] B. Castaing, J. Phys. (France) II **6**, 105 (1996).

[24] R. Benzi, L. Biferale, S. Ciliberto, M. Struglia, and R. Tripiccione, Physica D **96**, 162 (1996).
[25] L. M. Smith and V. Yakhot, Phys. Rev. Lett. **71**, 352 (1993).
[26] R. Kraichnan, Phys. Fluids **10**, 1417 (1967).
[27] U. Frisch and P. L. Sulem, Phys. Fluids **27**, 1921 (1984).
[28] N. Zouari and A. Babiano, Physica D **76**, 318 (1994).
[29] V. Borue, Phys. Rev. Lett. **72**, 1475 (1994).
[30] J. C. Vassilicos, in *Topological Aspects of the Dynamics of Fluids and Plasmas*, edited by H. K. Moffatt, G. M. Zaslavsky, M. Tabor, and P. Comte (Kluwer, Dordrecht, 1992), pp. 427–442.
[31] A. Vincent and M. Meneguzzi, J. Fluid Mech. **225**, 1 (1991).
[32] Z-S. She and E. C. Waymire, Phys. Rev. Lett. **74**, 262 (1995).
[33] P. Frick, B. Dubrulle, and A. Babiano, Phys. Rev. E **51**, 6 (1995); **51**, 5582 (1995).
[34] R. Sadourny and C. Basdevant, J. Atmos. Sci. **42**, 1353 (1985).
[35] A. Babiano, C. Basdevant, P. Le Roy, and R. Sadourny, J. Fluid Mech. **214**, 535 (1990).
[36] B. Dubrulle and F.-M. Bréon (unpublished).